Inorganica Chimica Acta 397 (2013) 75–82

Contents lists available at SciVerse ScienceDirect

Inorganica Chimica Acta

journal homepage: www.elsevier.com/locate/ica

Solvent- and temperature-driven synthesis of three Cd(II) coordination polymers based on 3,3′-azodibenzoic acid ligand: Crystal structures and luminescent properties

Lei-Lei Liu *, Lin Liu, Jun-Jie Wang

College of Chemistry and Chemical Engineering, Anyang Normal University, Anyang 455000, Henan, PR China

ARTICLE INFO

Article history:
Received 10 October 2012
Received in revised form 24 November 2012
Accepted 26 November 2012
Available online 3 December 2012

Keywords:
Solvent and temperature effects
3,3′-Azodibenzoic acid
Cd(II) coordination polymers
Crystal structure
Photoluminescent properties

ABSTRACT

Solvothermal reactions of $Cd(OAc)_2{\cdot}2H_2O$ with 3,3′-azodibenzoic acid (H_2L) in *N*,*N*′-dimethylformamide (DMF) or DMF/MeOH at 100 °C or 120 °C gave rise to three cadmium(II) coordination polymers $\{[CdL(DMF)_2]{\cdot}0.5DMF\}_n$ (**1**), $[CdL(DMF)(MeOH)]_n$ (**2**) and $\{[Cd_3L_3(DMF)_4]{\cdot}0.5DMF\}_n$ (**3**). Complexes **1**–**3** were characterized by elemental analysis, IR, powder X-ray diffraction and single-crystal X-ray diffraction. In **1**–**3**, dinuclear $[Cd_2L_4(DMF)_4]$ (**1**) or $[Cd_2L_4(DMF)_2(MeOH)_2]$ (**2**) unit and trinuclear $[Cd_3L_6(DMF)_4]$ (**3**) unit acts as a four-connecting node to link its equivalent ones *via* sharing L ligands to form 2D layers, which are further connected through the $C{-}H{\cdots}\pi$ (**1**) or hydrogen-bonding interactions (**2**–**3**) to afford 3D networks with the $4^{12}6^3$ topology. The network of **1** allows other one to be penetrated for the formation of twofold interpenetrating pcu net. The formation of **1**–**3** provided an interesting insight into solvent and temperature effects on the construction of coordination polymers under solvothermal conditions. In addition, the photoluminescent properties of **1**–**3** in solid state at ambient temperature were also investigated.

1. Introduction

The rational design and assembly of metal–organic frameworks (MOFs) have attracted much more attention in past few decades owing to their intriguing topologies and crystal packing motifs [1] as well as potential applications in gas storage/adsorption [2], catalysis [3], separations [4], drug delivery [5] and so on. Crystal engineering affords us a powerful tool for the design and construction of coordination frameworks [6]. And chemists and material scientists have been focusing their research on exploring the correlation between structures and functions of crystalline materials from 1990s, and huge efforts toward understanding the structural diversities and fascinating topologies associated with coordination polymers have promoted many meaningful results [7]. Generally, it is viable to select appropriate metal centers and organic linkers to form networks with predetermined structures and desired properties. However, in real chemical reactions, the environments, such as pH value, solvent, temperature, and reagent concentration, have an unpredictable impact on the crystallization of MOFs [8,9]. Minor changes of such environmental factors may lead to different architectures originated from differences in atomic connectivity or network catenation [10]. Solvent as one of the important factor often directly or indirectly influences the coordination behavior of the metal ions: it participates in the coordinated reactions or influences the overall frameworks without participating in coordination [11]. As for temperature, its effect on forming the coordination polymers has been intensively explored, and some reports described how the reaction temperature affects the generation of different coordination polymers [12]. However, the studies of solvent and temperature factors acting on the same reaction components are rare [13].

On the other hand, azobenzenecarboxylic compounds such as azobenzene-dicarboxylic, azobenzene-tricarboxylic and azobenzene-tetracarboxylic acids were utilized to construct functional MOFs [14]. For example, Yaghi used 4,4′-azodibenzoic acid (H_2ADB) to react with $Tb(NO_3)_3{\cdot}5H_2O$ to get an interpenetrating network of $\{Tb_2(ADB)_3[(CH_3)_2SO]_4{\cdot}16[(CH_3)_2SO]\}_n$ with large free volume [15]. Recently, Lu and co-workers reported three porous MOFs constructed by using azobenzene-3,5,4′-tricarboxylic acid (H_3ABTC) and $Cd(NO_3)_2{\cdot}4H_2O/MnCl_2{\cdot}4H_2O$ as building blocks [14b]. Qiu et al. used 3,3′,5,5′-azobenzenetetracarboxylic acid (H_4ABTC) as a building block to construct three 3D microporous MOFs with NbO and PtS topologies, which show hydrogen storage and luminescent properties [16]. To our best knowledge, the coordination chemistry of 3,3′-azodibenzoic acid has attracted little attention, with exception of the recent report on the assembly of 3,3′-azodibenzoic acid with $Zn(OAc)_2/Co(OAc)_2/PbI_2$ and 1,10-phenanthroline [14a]. Moreover, studies engaged in solvent- and/or

---

* Corresponding author. Fax: +86 372 2900040.
E-mail address: liuleileimail@163.com (L.-L. Liu).

0020-1693/$ - see front matter © 2012 Elsevier B.V. All rights reserved.
http://dx.doi.org/10.1016/j.ica.2012.11.021

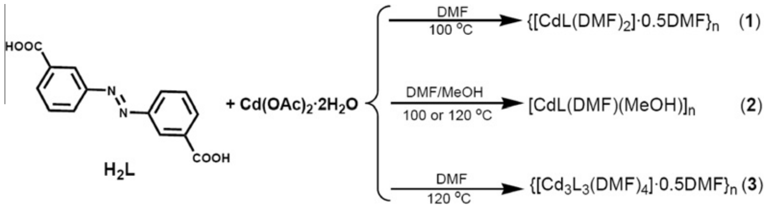

Scheme 1.

temperature-dependent construction of coordination polymers containing 3,3′-azodibenzoic acid have not been reported so far. In this work, the solvothermal reactions of $Cd(OAc)_2{\cdot}2H_2O$ with 3,3′-azodibenzoic acid (H_2L) in DMF or DMF/MeOH at 100 or 120 °C gave rise to three Cd(II) coordination polymers with different structures $\{[CdL(DMF)_2]{\cdot}0.5DMF\}_n$ (**1**), $[CdL(DMF)(MeOH)]_n$ (**2**) and $\{[Cd_3L_3(DMF)_4]{\cdot}0.5DMF\}_n$ (**3**). The results indicated that solvent and temperature significantly affect the formation of these cadmium(II) coordination polymers. Herein we describe the solvent- and temperature-oriented reactions along with the crystal structures and photoluminescent properties of **1**–**3** (Scheme 1).

2. Experimental

2.1. Materials and general methods

3,3′-azodibenzoic acid (H_2L) was prepared according to the literature methods [17]. All chemicals and reagents were obtained from commercial sources and used as received. The IR spectra were recorded as KBr pellets on a Varian 800 FT-IR spectrometer in the 4000–400 cm^{-1} region. Powder X-ray diffraction (PXRD) measurements were performed on a Bruker Ultima III X-ray diffractometer with Cu Kα (λ = 1.5418 Å). Luminescent spectra were recorded with a Rigaku RIX 2000 fluorescence spectrophotometer.

2.2. Synthesis of complexes **1**–**3**

2.2.1. $\{[CdL(DMF)_2]{\cdot}0.5DMF\}_n$ (**1**)

A mixture of $Cd(OAc)_2{\cdot}2H_2O$ (13 mg, 0.05 mmol), H_2L ligand (7 mg, 0.025 mmol), and DMF (4 mL) was sealed in a 10 mL Pyrex glass tube and heated at 100 °C for 4 days, then cooled to room temperature at a rate of 5 °C h^{-1}. The yellow blocks of **1** were collected and washed thoroughly with DMF and dried in air. Yield: 11 mg (40%, based on Cd). *Anal.* Calc. for $C_{21.5}H_{23}N_{4.5}CdO_{6.5}$: C, 46.04; H, 4.13; N, 11.24. Found: C, 46.50; H, 4.38; N, 11.01%. IR (KBr disc): 3352 (m), 3272 (m), 3071 (w), 2931 (w), 1652 (s), 1591 (s), 1549 (s), 1475 (m), 1439 (m), 1394 (s), 1311 (w), 1253 (w), 1225 (w), 1155 (m), 1109 (m), 1075 (m), 936 (w), 811 (m), 781 (m), 684 (m), 538 (w), 411 (w) cm^{-1}.

2.2.2. $[CdL(DMF)(MeOH)]_n$ (**2**)

Compound **2** (orange flakes) was prepared in the same way as **1**, except using mixed solvent DMF/MeOH (4 mL, 1:1, V/V) instead of solvent DMF (4 mL). Yield: 8 mg (35%, based on Cd). *Anal.* Calc. for $C_{18}H_{18}N_3CdO_6$: C, 44.60; H, 3.74; N, 8.67. Found: C, 44.21; H, 4.13; N, 8.55%. IR (KBr disc): 3386 (m), 3300 (m), 3065 (w), 2932 (w), 1645 (s), 1592 (s), 1545 (s), 1477 (w), 1398 (s), 1221 (w), 1154 (w), 1111 (m), 1075 (w), 1024 (m), 936 (w), 866 (w), 810 (m), 779 (m), 680 (m), 536 (w), 416 (w) cm^{-1}.

Table 1
Summary of crystallographic data for **1**–**3**.

Compound	1	2	3
Empirical formula	$C_{43}H_{44}Cd_2N_9O_{13}$	$C_{18}H_{19}CdN_3O_6$	$C_{55.5}H_{38}Cd_3N_{10.5}O_{16.5}$
Formula weight	1119.69	485.77	1453.19
Crystal system	monoclinic	monoclinic	triclinic
Space group	$C2/c$	$P2_1/c$	$P\bar{1}$
a (Å)	28.608(6)	9.3878(19)	11.476(2)
b (Å)	9.3713(19)	10.051(2)	12.089(2)
c (Å)	20.496(4)	21.113(4)	12.476(3)
α (°)			01.21(3)
β (°)	119.26(3)	102.85(3)	95.16(3)
γ (°)			106.49(3)
V (Å^3)	4794(2)	1942.3(7)	1608.5(7)
Z	4	4	1
T (K)	296(2)	296(2)	296(2)
ρ_{calc} (g/cm^3)	1.551	1.661	1.500
$F(000)$	2260.0	976.0	720.5
μ (Mo Kα, mm^{-1})	0.958	1.164	1.053
Total reflections	24430	47686	16521
Unique reflections	4218	4632	5671
No. of observations	3410	3887	4837
No. of parameters	319	255	393
R_1[a]	0.0613	0.0471	0.0388
wR_2[b]	0.1582	0.1164	0.1171
Goodness-of-fit (GOF)[c]	1.139	1.068	0.972

[a] $R_1 = \Sigma||F_o| - |F_c||/\Sigma|F_o|$.

[b] $wR_2 = \{\Sigma w(F_o^2 - F_c^2)^2/\Sigma w(F_o^2)^2\}^{1/2}$.

[c] $GOF = \{\Sigma w(F_o^2 - F_c^2)^2/(n - p)\}^{1/2}$, where n = number of reflections and p = total numbers of parameters refined.

2.2.3. *{[$Cd_3L_3(DMF)_4$]·0.5DMF}$_n$ (**3**)*

Compound **3** (orange blocks) was prepared in a manner similar to that described for **1**, using the same components in the same molar ratio except the reaction temperature was fixed at 120 °C. Yield: 13 mg (46%, based on Cd). *Anal.* Calc. for $C_{55.5}H_{51}N_{10.5}Cd_3O_{16.5}$: C, 45.46; H, 3.51; N, 10.03. Found: C, 45.15; H, 3.08; N, 10.35%. IR (KBr disc): 3383 (m), 3302 (m), 3101 (w), 2957 (w), 1672 (s), 1611 (s), 1565 (s), 1500 (m), 1469 (m), 1420 (s), 1335 (w), 1276 (w), 1250 (w), 1180 (m), 1141 (m), 1100 (m), 960 (w), 841 (m), 801 (m), 721 (m), 569 (w), 440 (w) cm^{-1}.

2.3. X-ray crystallographic studies

Single crystals of **1**–**3** were obtained directly from the above preparations. All measurements were made on a Bruker Smart Apex-II CCD area detector by using graphite monochromated Mo Kα (λ = 0.071073 nm). These crystals were mounted on glass fibers at 296 K for **1**–**3**. Diffraction data were collected at *f* and ω modes with a detector distance of 35 mm to the crystals. Cell parameters were refined by using the program Bruker SAINT. The collected data were reduced by using the program Bruker SAINT A, and the absorption corrections (multi-scan) were applied. The reflection data were also corrected for Lorentz and polarization effects.

Table 2
Selected bond lengths (Å) and angles (°) for **1**–**3**.[a]

*Complex **1***			
Cd(1)–O(3)	2.257(6)	Cd(1)–O(6)	2.316(9)
Cd(1)–O(1A)	2.320(5)	Cd(1)–O(5)	2.325(7)
Cd(1)–O(2)	2.335(5)	Cd(1)–O(1)	2.486(6)
Cd(1)–O(4)	2.568(6)	N(1)–N(1B)	1.235(13)
N(2)–N(2C)	1.234(14)	O(3)–Cd(1)–O(6)	91.1(3)
O(3)–Cd(1)–O(1A)	91.6(2)	O(6)–Cd(1)–O(1A)	86.4(3)
O(3)–Cd(1)–O(5)	90.0(2)	O(6)–Cd(1)–O(5)	171.8(3)
O(1A)–Cd(1)–O(5)	101.6(2)	O(3)–Cd(1)–O(2)	140.9(2)
O(6)–Cd(1)–O(2)	88.4(3)	O(1A)–Cd(1)–O(2)	127.32(19)
O(5)–Cd(1)–O(2)	85.7(2)	O(3)–Cd(1)–O(1)	165.30(18)
O(6)–Cd(1)–O(1)	90.8(3)	O(1A)–Cd(1)–O(1)	73.92(19)
O(5)–Cd(1)–O(1)	90.2(2)	O(2)–Cd(1)–O(1)	53.76(18)
O(3)–Cd(1)–O(4)	53.0(2)	O(6)–Cd(1)–O(4)	85.4(3)
O(1A)–Cd(1)–O(4)	143.5(2)	O(5)–Cd(1)–O(4)	88.8(2)
O(2)–Cd(1)–O(4)	87.96(19)	O(1)–Cd(1)–O(4)	141.65(18)
N(1B)–N(1)–C(4)	115.1(8)	N(2C)–N(2)–C(11)	113.3(9)
*Complex **2***			
Cd(1)–O(4A)	2.214(4)	Cd(1)–O(6)	2.266(4)
Cd(1)–O(3B)	2.301(4)	Cd(1)–O(5)	2.341(5)
Cd(1)–O(2)	2.346(4)	Cd(1)–O(1)	2.377(4)
N(1)–N(2)	1.246(6)	O(4A)–Cd(1)–O(6)	124.28(14)
O(4A)–Cd(1)–O(3B)	106.38(15)	O(6)–Cd(1)–O(3B)	85.78(15)
O(4A)–Cd(1)–O(5)	80.27(16)	O(6)–Cd(1)–O(5)	84.19(15)
O(3B)–Cd(1)–O(5)	169.92(14)	O(4A)–Cd(1)–O(2)	135.24(15)
O(6)–Cd(1)–O(2)	96.05(14)	O(3B)–Cd(1)–O(2)	93.99(15)
O(5)–Cd(1)–O(2)	86.07(15)	O(4A)–Cd(1)–O(1)	85.92(13)
O(6)–Cd(1)–O(1)	149.73(13)	O(3B)–Cd(1)–O(1)	87.36(15)
O(5)–Cd(1)–O(1)	100.84(17)	O(2)–Cd(1)–O(1)	55.08(12)
N(2)–N(1)–C(6)	112.9(5)	N(1)–N(2)–C(8)	113.9(5)
*Complex **3***			
Cd(1)–O(5)	2.188(4)	Cd(1)–O(3)	2.231(4)
Cd(1)–O(8)	2.272(14)	Cd(1)–O(7)	2.302(4)
Cd(1)–O(1A)	2.358(4)	Cd(1)–O(2A)	2.381(3)
Cd(2)–O(6B)	2.232(3)	Cd(2)–O(4B)	2.268(3)
Cd(2)–O(2A)	2.340(3)	N(1)–N(2)	1.246(6)
N(3)–N(3D)	1.238(8)	O(5)–Cd(1)–O(3)	96.58(15)
O(1A)–Cd(1)–O(2A)	55.18(11)	O(7)–Cd(1)–O(2A)	156.97(14)
O(5)–Cd(1)–O(8)	83.8(4)	O(3)–Cd(1)–O(8)	170.8(4)
O(5)–Cd(1)–O(7)	98.69(15)	O(3)–Cd(1)–O(7)	85.35(15)
O(8)–Cd(1)–O(7)	85.5(4)	O(5)–Cd(1)–O(1A)	158.56(13)
O(3)–Cd(1)–O(1A)	91.22(16)	O(8)–Cd(1)–O(1A)	91.6(4)
O(7)–Cd(1)–O(1A)	101.83(14)	O(5)–Cd(1)–O(2A)	104.29(12)
O(3)–Cd(1)–O(2A)	93.35(13)	O(8)–Cd(1)–O(2A)	95.4(4)
O(6B)–Cd(2)–O(4B)	91.33(14)	O(6B)–Cd(2)–O(2C)	88.01(14)
O(4B)–Cd(2)–O(2C)	94.50(12)	O(6B)–Cd(2)–O(2A)	91.99(14)
O(2C)–Cd(2)–O(4)	85.50(12)	O(6B)–Cd(2)–O(6)	180.000(1)
O(4B)–Cd(2)–O(6)	88.67(14)	N(3D)–N(3)–C(16)	114.8(5)
N(2)–N(1)–C(6)	113.1(4)	N(1)–N(2)–C(8)	114.2(4)

[a] Symmetry codes for **1**: (A) $-x + 1/2, -y + 1/2, -z$; (B) $-x, -y, -z$; (C) $-x, -y + 1, -z - 1$; for **2**: (A) $x + 1, -y + 1/2, z - 1/2$; (B) $-x + 1, y + 1/2, -z + 3/2$; for **3**: (A) $x, y, z + 1$; (B) $-x + 1, -y + 1, -z + 2$; (C) $-x + 1, -y + 1, -z + 1$; (D) $-x, -y, -z + 1$.

The crystal structures of **1**–**3** were solved by direct method refined on F^2 by full-matrix least-squares techniques with the SHELXTL-97 program [18]. In **3**, one coordinated DMF solvent molecule was found to be disordered over two positions with an occupancy factor of 0.700/0.300 for O8/O8A, N5/N5A, C25–C27/C25A–C27A. Hydrogen atoms of the DMF solvent molecules in **1** (C21–C23) and **3** (C25–C30) were not located. All other H atoms in **1**–**3** were placed in geometrically idealized positions and constrained to ride on their parent atoms. The site occupation factors for O7, N5, C21–C23 atoms in **1** and O9, N6, C28–C30 atoms in **3** were fixed at 0.5 and 0.25, respectively, which were maybe due to the partial evaporation of the DMF solvent molecules. A summary of the key crystallographic information for **1**–**3** is tabulated in Table 1 and their selected bond lengths and angles are given in Table 2.

3. Results and discussion

3.1. Synthesis consideration and general characterization

In all solvothermal reactions reported here, the molar ratio of $Cd(OAc)_2·2H_2O$ to H_2L was kept at 2:1. Reactions of $Cd(OAc)_2·2H_2O$ with H_2L in DMF for four days at 100 °C and cooled to ambient temperature at a rate of 5 °C h^{-1} produced yellow crystals of **1** (40% yield). When the reaction temperature was raised up to 120 °C, the orange crystals of **3** (46% yield) were generated through the similar manners to those described for **1**. Analogous reactions except using mixture solvent DMF/MeOH (4 mL, 1:1, V/V) instead of solvent DMF (4 mL, **1** and **3**) at 100 °C afforded orange crystals of **2** (35% yield). Notice that even the reaction temperature was raised up to 120 °C, but only compound **2** was obtained. We also attempted to crystallize at other mixture solvents, but always failed to form any crystals. When the reaction temperature fell to 90 °C, crystals of **1** and **2** were obtained with relatively lower yields. However, increasing the temperature to 140 °C, only orange precipitates were isolated and the PXRD pattern was inconsistent with those of **1**–**3**.

Compounds **1**–**3** were stable towards oxygen and moisture, and almost insoluble in common organic solvents. The IR spectra of **1**–**3** showed peaks in the range of 1645–1672 and 1394–1420 cm^{-1}, which is indicative of the existence of coordinated carboxylic groups [19a]. The middle peaks in the range of 1591–1611 cm^{-1} were assigned to the asymmetric N=N vibration of complexes **1**–**3** [8g]. The identities of **1**–**3** were further confirmed by single-crystal diffraction analysis. The PXRD patterns of **1**–**3** were matched with the simulated patterns generated from their single crystals data (Fig. S1).

3.2. Description of the crystal structures

3.2.1. *{[CdL(DMF)$_2$]·0.5DMF}$_n$ (**1**)*

Compound **1** crystallizes in the monoclinic space group *C*2/*c*, and its asymmetric unit contains one [CdL(DMF)$_2$] molecule, half of a DMF solvent molecule. As shown in Fig. 1a, each Cd atom adopts a pentagonal bipyramidal coordination geometry, is coordinated by four O (O1, O2, O3 O4) atoms of chelating carboxylate groups from two different L ligands, one O (O1A) atom of bridging carboxylate groups from third L ligands and two O (O5, O6) atoms from two different DMF molecules. The carboxylate groups of the L

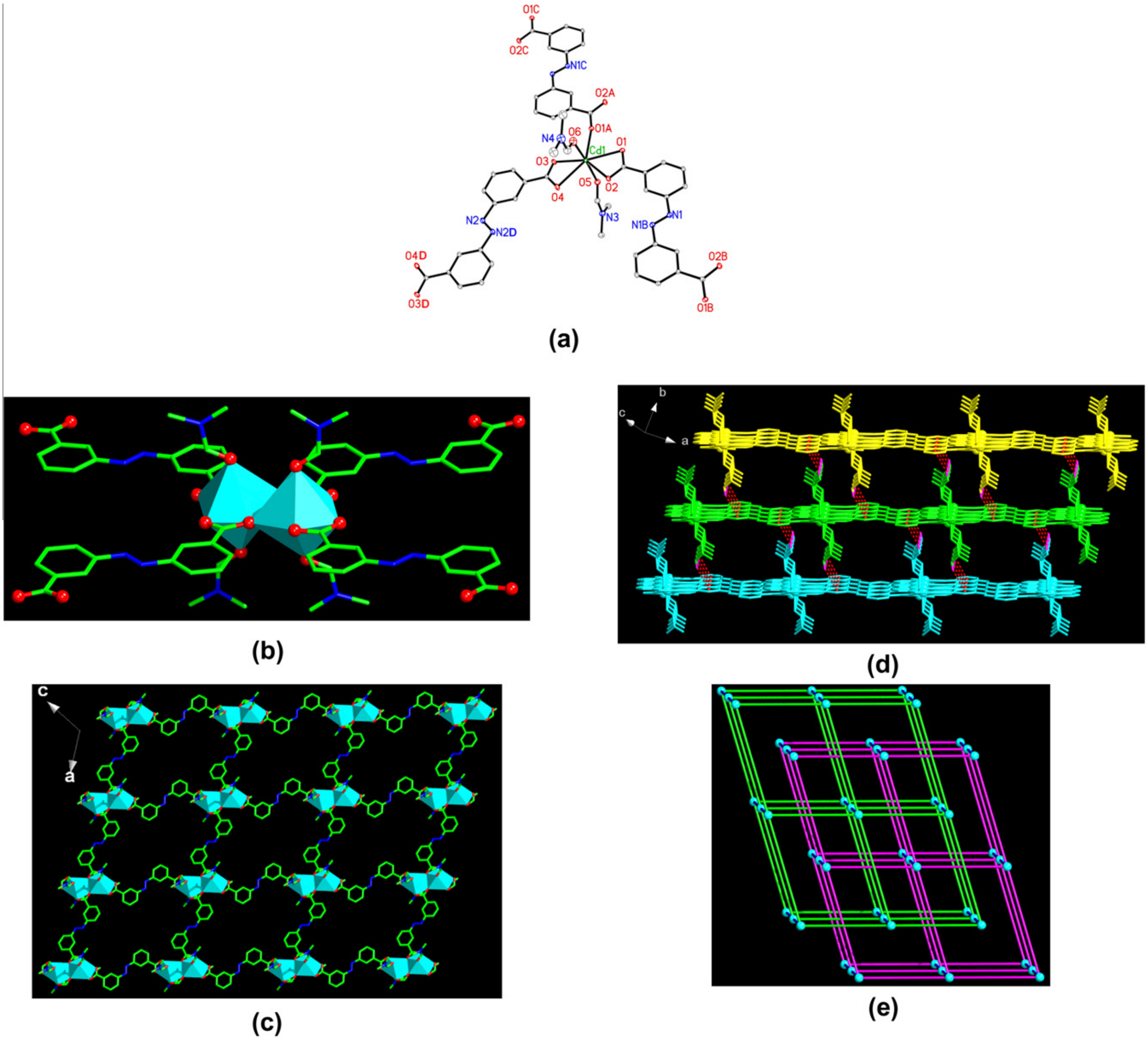

Fig. 1. (a) View of the coordination environments of Cd center in **1** with labeling schemes. Symmetry codes: (A) $-x + 1/2$, $-y + 1/2$, $-z$; (B) $-x$, $-y$, $-z$; (C) $-x$, $-y + 1$, $-z - 1$; (D) $x + 1/2$, $y + 1/2$, z. (b) View of one dinuclear $[Cd_2L_4(DMF)_4]$ unit of **1**. (c) View of a 2D layer in **1** extending along the *ac* plane. (d) View of a 3D structure in **1** looking along the *c* axis. (e) View of the twofold interpenetration model in **1**. Each single net represents a pcu topology with a Schläfli symbol $4^{12}6^3$. Atom color codes: Cd, cyan pentagonal bipyramid; O, red; N, blue; and C, green. All H atoms except those related to H-bonding interactions and uncoordinated DMF molecules are omitted for clarity. (For interpretation of the references to color in this figure legend, the reader is referred to the web version of this article.)

ligand in **1** display the chelating and chelating/bridging coordination modes. Cd1 and its symmetry-related Cd1A are bridged by two L ligands to generate a dinuclear $[Cd_2L_4(DMF)_4]$ unit (Fig. 1b). Each dinuclear unit serves as a planar fourfold node, which links its four equivalent ones *via* sharing L ligands to form a 2D layer with parallelogram meshes extending along the *ac* plane (Fig. 1c). Each mesh in this 2D layer has a dimension of 15.05×15.19 Å^2. Furthermore, this layer is connected to neighboring layers *via* H···π interactions [C19A···*Cg*(x, $y + 1$, z) = 2.965 Å, where *Cg* is the centroid of the C2/C3/C4/C5/C6/C7 ring], thereby completing a 3D network extending along the *ab* plane (Fig. 1d) [19b]. This network was big enough to allow the other network to penetrate to form a twofold interpenetrating pcu net with a Schläfli symbol of $4^{12}6^3$ (Fig. 1e) [20]. Although the interpenetration in **1** occurs, there is still approximately 11.4% of the crystal volume accessible to the solvents [21].

3.2.2. $[CdL(DMF)(MeOH)]_n$ (**2**)

Compound **2** crystallizes in the monoclinic space group $P2_1/c$, and its asymmetric unit contains one [CdL(DMF)(MeOH)] molecule. The coordination environment of Cd^{2+} in **2** is different from that of in **1**. Each Cd atom in **2** adopts a disordered octahedral coordination geometry, is coordinated by two O (O3A, O4B) atoms of two bridging carboxylate groups from two L ligands, two O (O1, O2) atoms of one chelating carboxylate groups from third L ligands as well as two O (O5, O6) atoms from DMF and MeOH molecules (Fig. 2a). The mean Cd–O bond length (2.307(5) Å) is shorter than that of **1** (2.372(4) Å), while the N=N (1.246(6) Å) bond length of **2** is slightly longer than that observed in **1** (1.234(13) Å, Table 2). In contrast, the carboxylate groups of the L ligand in **2** display the bridging and chelating coordination modes. Two [CdL(DMF)(MeOH)] subunits are bridged by two L ligands to generate a dinuclear $[Cd_2L_4(DMF)_2(MeOH)_2]$ unit (Fig. 2b). Each dinuclear $[Cd_2L_4(DMF)_2(MeOH)_2]$ unit also serves as a fourfold node, which

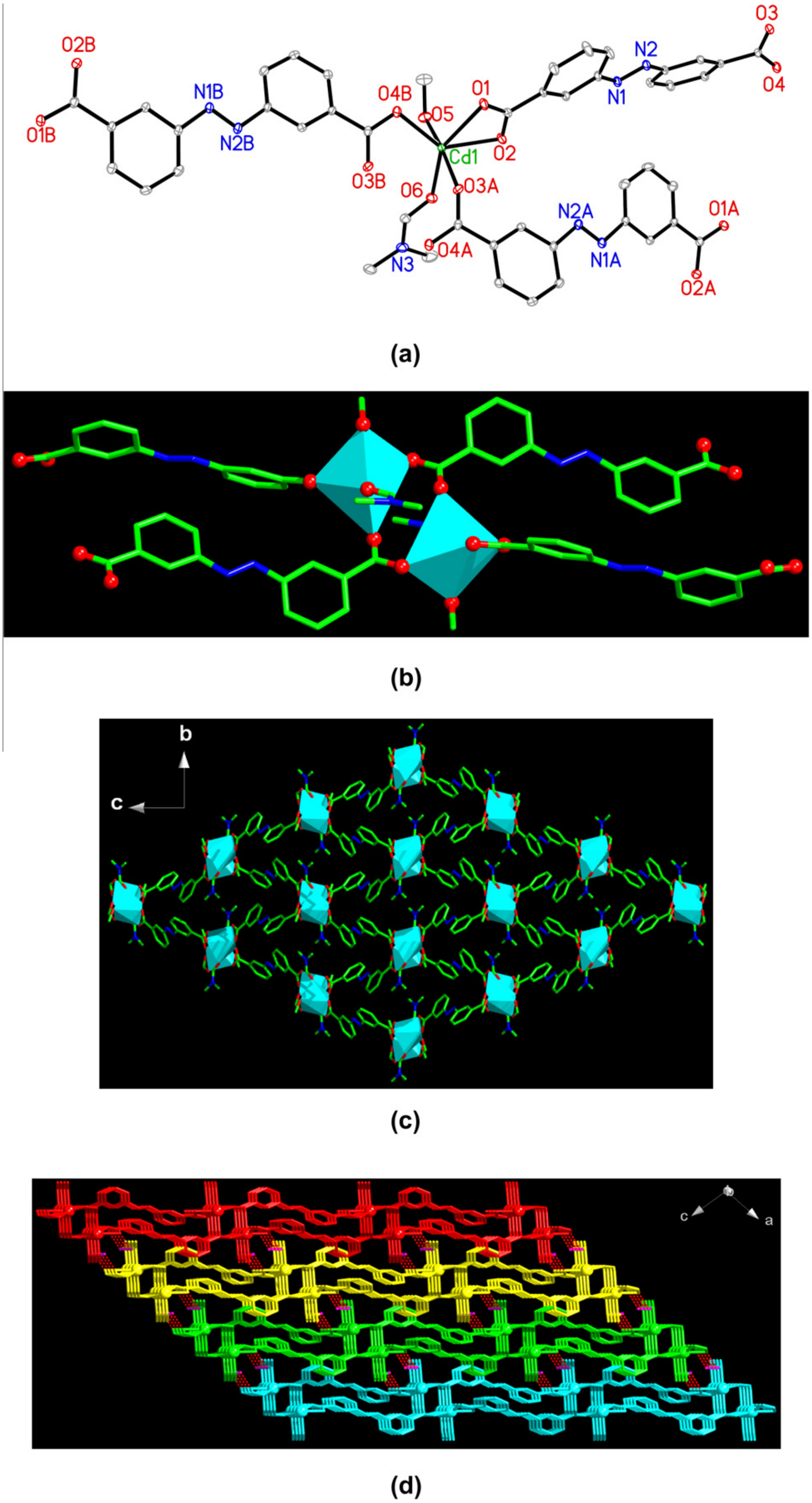

Fig. 2. (a) View of the coordination environments of Cd center in **2** with labeling schemes. Symmetry codes: (A) $1 - x, -y + 1/2, -z + 3/2$; (B) $x + 1, -y + 1/2, z - 1/2$; (b) View of one dinuclear $[Cd_2L_4(DMF)_2(MeOH)_2]$ unit of **2**. (c) View of a 2D network in **2** extending along the *bc* plane. (d) View of a 3D structure in **2** looking along the *b* axis. Atom color codes: Cd, cyan pentagonal bipyramid; O, red; N, blue; and C, green. All H atoms except those related to H-bonding interactions and DMF molecules are omitted for clarity. (For interpretation of the references to color in this figure legend, the reader is referred to the web version of this article.)

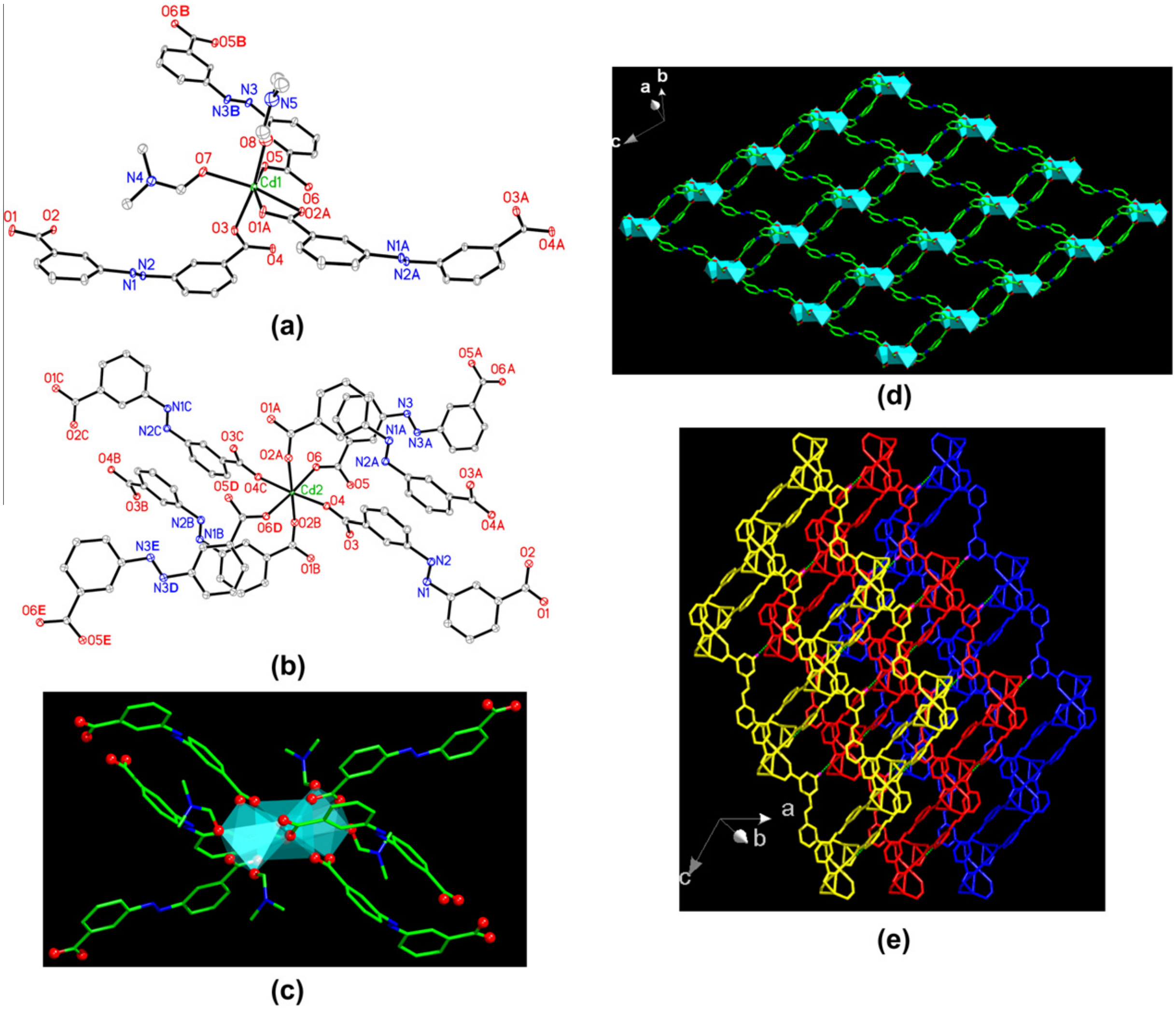

Fig. 3. (a and b) View of the coordination environments of Cd1 and Cd2 centers in **3** with labeling schemes. Symmetry codes: (A) $-x$, $-y$, $-z+1$; (B) x, y, $z+1$; (C) $-x+1$, $-y+1$, $-z+1$; (D) $-x+1$, $-y+1$, $-z+2$; (E) $x+1$, $y+1$, $z+1$. (c) View of one trinuclear $[Cd_3L_6(DMF)_4]$ unit of **3**. (d) View of a 2D network in **3** extending along the *bc* plane. (e) View of a 3D structure in **3** looking along the *b* axis. Atom color codes: Cd, cyan; O, red; N, blue; and C, green. All H atoms except those related to H-bonding interactions and DMF molecules are omitted for clarity. (For interpretation of the references to color in this figure legend, the reader is referred to the web version of this article.)

links its four equivalent ones *via* sharing four L ligands to form a 2D network with parallelogram meshes (13.81 × 16.10 Å^2) extending along the *bc* plane (Fig. 2c). Each 2D network is further interconnected with neighboring ones *via* intermolecular hydrogen bond between the coordinated MeOH molecule and a CO_2^- group in other network (O5–H5A···2, 2.681 Å, Table S1) to form a 3D structure extending along the *ac* plane (Fig. 2d). If the $[Cd_2L_4(DMF)_2(MeOH)_2]$ unit is considered as six-connecting nodes, the whole structure of **2** also display a $4^{12}6^3$ topological net (Fig. S2). The PLATON program analysis of **2** suggests that there is no residual solvent accessible void in the unit cell.

3.2.3. $\{[Cd_3L_3(DMF)_4]\cdot 0.5DMF\}_n$ (**3**)

Compound **3** crystallizes in the triclinic space group $P\bar{1}$, and its asymmetric unit contains half a $[Cd_3L_3(DMF)_4]$ unit, one quarter of DMF solvent molecule. The coordination environment of Cd(II) in **3** is different from that of in **1**, but is similar with that of in **2**. Cd1 atom is six-coordinated by two O (O3, O5) atoms of bridging carboxylate groups from two different L ligands, two O (O1A, O2A) atoms of chelating carboxylate groups from third L ligands, and two O (O7, O8) atoms from two different DMF molecules (Fig. 3a). Cd2 atom is also octahedrally coordinated by six O (O3, O5) atoms of bridging carboxylate groups from six L ligands (Fig. 3b). For Cd1 and Cd2, their mean Cd–O bond length (2.285(5) Å) is shorter than that of **1** (2.372(4) Å) and **2** (2.307(5) Å). And the mean N=N (1.242(7) Å) bond length of **3** is comparable that of **2** (1.246(6) Å), but is slightly longer than that observed in **1** (1.234(13) Å, Table 2). The carboxylate groups of the L ligand in **3** show the bridging and chelating/bridging coordination modes. Cd2, Cd1 and its symmetry-related Cd1A are bridged by four L ligands to generate a trinuclear $[Cd_3L_6(DMF)_4]$ unit (Fig. 3c). The trinuclear unit links its neighboring four equivalent ones *via* sharing L ligands to form a 2D network with parallelogram grids (12.48 × 16.63 Å^2) extending along the *bc* plane (Fig. 3d). Adjacent networks are interconnected by H-bonding interactions between O atoms of carboxylate groups and H atoms of the phenyl group with C18 [C18–H18···O1, 3.342 Å, Table S1] to afford a 3D architecture (Fig. 3e) with the effective solvent accessible volume of 214.3 Å^3 per unit cell (13.3% of the total cell volume) filled with DMF solvent molecules. Similar to that of in **1**–**2**, compound **3** also show a $4^{12}6^3$ topological structure (based on each $[Cd_3L_6(DMF)_4]$ unit as a six-connecting node) (Fig. S3).

The formation of different structures of **1**–**3** at different solvents and temperatures deserves comments. Compounds **1** and **3** were produced in DMF at 100 °C and 120 °C, respectively, while compound **2** was generated in the mixed solvent DMF/MeOH at

100 °C. As described earlier in this article, the structures of **1**–**3** are greatly different in the following aspects. Firstly, Cd atoms in **1** adopt pentagonal bipyramidal coordination geometry, while those of in **2**–**3** show octahedral coordination geometry. Secondly, compounds **1**–**2** adopted a dinuclear $[Cd_2L_4(DMF)_4]$ (**1**) or $[Cd_2L_4(DMF)_2(MeOH)_2]$ (**2**) unit while compound **3** had a trinuclear $[Cd_3L_6(DMF)_4]$ unit, which implied that higher nuclear units (**3**) may be stable than the lower nuclear units (**1**) at the higher temperature [22]. Moreover, each dinuclear or trinuclear unit serves as a fourfold node, which links its four equivalent ones *via* sharing four (**1**–**2**) or six (**3**) L ligands to generate a 3D structure. Thirdly, compound **1** possessed one twofold interpenetrating 3D network while **2**–**3** hold non-interpenetrating 3D structures. This suggests that at lower temperatures the interpenetrating 3D structures of **1** may be not stable than the non-interpenetrating 3D networks of **3** and may be converted directly into the structures of **3**, which was consistent with those reported previously [23]. Fourthly, compounds **1**–**3** exhibited different crystal volume accessible to the solvents of **1** (11.4%), **2** (0%) and **3** (13.4%), respectively. The difference between **1** and **2** indicated that solvent did work in the construction of polymers **1** and **2**. From the above-mentioned comparison, it is noted that the solvent and temperature effects in this study greatly affected the coordination geometry of Cd atoms, the formation of different Cd-containing units and the whole structures of these compounds.

3.3. Photoluminescent properties

The photoluminescent properties of **1**–**3** in solid state at room temperature were studied (Fig. S4). Ligand H_2L did not show photoluminescent property. Excitation of **1**–**3** at 470 nm, 473 nm and 463 nm resulted in a strong emission band at 546 nm, 557 nm and 535 nm, respectively. The emissions for **1**–**3** may be assigned to be the metal-to-ligand charge transfer (MLCT) with electrons being transferred from Cd(II) centers to the unoccupied π^* orbitals of the carboxylic groups [24].

4. Conclusions

In this paper, we have demonstrated the formation of three Cd(II) coordination polymers **1**–**3** from the solvothermal reactions of $Cd(OAc)_2 \cdot 2H_2O$ with H_2L in DMF or DMF/MeOH at 100 or 120 °C. Compounds **2** and **3** both have unusual 3D coordination architectures with a Schläfli symbol of $4^{12}6^3$ based on the dinuclear $[Cd_2L_4(DMF)_2(MeOH)_2]$ (**2**) units and trinuclear $[Cd_3L_6(DMF)_4]$ (**3**) units, while compound **1** holds a novel 3D twofold interpenetrating network based on the dinuclear $[Cd_2L_4(DMF)_4]$ units and also exhibits a $4^{12}6^3$ topological structure. According to the aforementioned X-ray structural analysis, it is noted that the L ligand shows rich conformational changes when it binds to Cd centers. And its carboxyl groups can have different coordination modes (bridging, chelating, and/or bridging/chelating). Evidently, the reaction solvent and temperature played an important role in the formation of these cadmium(II) coordination polymers with different structures. This work highlights a delicate solvent and temperature induced assembly in crystal engineering of functional coordination polymers, which would lead to new compounds with interesting structures and properties.

Acknowledgement

We are grateful to the National Natural Science Foundation of China (21205003) and the Research Start-Up Fund for New Staff of Anyang Normal University (Grant No. 308772).

Appendix A. Supplementary material

Supplementary data associated with this article can be found, in the online version, at http://dx.doi.org/10.1016/j.ica.2012.11.021.

References

[1] (a) F.A. Cotton, C. Lin, C. Murillo, Acc. Chem. Res. 34 (2001) 759;
(b) O.R. Evans, W.B. Lin, Acc. Chem. Res. 35 (2002) 511;
(c) D. Gatteschi, R. Sessoli, Angew. Chem., Int. Ed. 42 (2003) 268;
(d) G. Férey, C. Mellot-Draznieks, C. Serre, F. Millange, Acc. Chem. Res. 38 (2005) 217;
(e) B. Moulton, M.J. Zaworotko, Chem. Rev. 101 (2001) 1629;
(f) S.L. James, Chem. Soc. Rev. 32 (2003) 276;
(g) J.P. Zhang, Y.B. Zhang, J.B. Lin, X.M. Chen, Chem. Rev. 112 (2012) 1001;
(h) W. Zhang, R.G. Xiong, Chem. Rev. 112 (2012) 1163.

[2] (a) X. Zhao, B. Xiao, A. Fletcher, K.M. Thomas, D. Bradshaw, M.J. Rosseinsky, Science 306 (2004) 1012;
(b) M. Eddaoudi, J. Kim, N. Rosi, D. Vodak, J. Wachter, M. O'Keeffe, O.M. Yaghi, Science 295 (2002) 469;
(c) L.J. Murray, M. Dincá, J.R. Long, Chem. Soc. Rev. 38 (2009) 1294;
(d) R.E. Morris, P.S. Wheatley, Angew. Chem., Int. Ed. 47 (2008) 4966;
(e) J.R. Li, R.J. Kuppler, H.C. Zhou, Chem. Soc. Rev. 38 (2009) 1477.

[3] (a) C.D. Wu, A. Hu, L. Zhang, W. Lin, J. Am. Chem. Soc. 127 (2005) 8940;
(b) P.M. Forster, A.K. Cheetham, Top. Catal. 24 (2003) 79;
(c) L. Ma, C. Abney, W. Lin, Chem. Soc. Rev. 38 (2009) 1248;
(d) J. Lee, O.K. Farha, J. Roberts, K.A. Scheidt, S.T. Nguyen, J.T. Hupp, Chem. Soc. Rev. 38 (2009) 1450.

[4] (a) V. Finsy, H. Verelst, L. Alaerts, D.E. De Vos, P.A. Jacobs, G.V. Baron, J.F.M. Denayer, J. Am. Chem. Soc. 130 (2008) 7110;
(b) R. Kitaura, K. Seki, G. Akiyama, S. Kitagawa, Angew. Chem., Int. Ed. 42 (2003) 428;
(c) D. Liu, J.P. Lang, B.F. Abarahams, J. Am. Chem. Soc. 133 (2011) 11042.

[5] P. Horcajada, C. Serre, M. Vallet-Regi, M. Sebban, F. Taulelle, G. Férey, Angew. Chem., Int. Ed. 45 (2006) 597.

[6] (a) B.F. Abrahams, P.A. Jackson, R. Robson, Angew. Chem., Int. Ed. 37 (1998) 2656;
(b) Y.F. Zhou, F.L. Jiang, D.Q. Yuan, B.L. Wu, R.H. Wang, Z.L. Lin, M.C. Hong, Angew. Chem., Int. Ed. 43 (2004) 5665;
(c) D. Liu, Z.G. Ren, H.X. Li, J.P. Lang, N.Y. Li, B.F. Abrahams, Angew. Chem., Int. Ed. 49 (2010) 4767.

[7] (a) O.K. Farha, C.D. Malliakas, M.G. Kanatzidis, J.T. Hupp, J. Am. Chem. Soc. 132 (2010) 950;
(b) M. Fujita, M. Tominaga, A. Hori, B. Therrien, Acc. Chem. Res. 38 (2005) 369;
(c) X.L. Zhao, H.Y. He, T.P. Hu, F.N. Dai, D.F. Sun, Inorg. Chem. 48 (2009) 8057;
(d) X.L. Wang, C. Qin, E.B. Wang, Y.G. Li, Z.M. Su, L. Xu, L. Carlucci, Angew. Chem., Int. Ed. 44 (2005) 5824;
(e) N.C. Gianneschi, M.S. Masar, C.A. Mirkin, Acc. Chem. Res. 38 (2005) 825;
(f) D. Liu, Y.J. Chang, J.P. Lang, CrystEngComm 13 (2011) 1851.

[8] (a) J.L. Du, T.L. Hu, J.R. Li, S.M. Zhang, X.H. Bu, Eur. J. Inorg. Chem. (2008) 1059;
(b) B. Xu, Z.J. Lin, L.W. Han, R. Cao, CrystEngComm 13 (2011) 440;
(c) Y.F. Han, X.Y. Li, L.Q. Li, C.L. Ma, Z. Shen, Y. Song, X.Z. You, Inorg. Chem. 49 (2010) 10781;
(d) J. Yang, G.D. Li, J.J. Cao, Q. Yue, G.H. Li, J.S. Chen, Chem. Eur. J. 13 (2007) 3248;
(e) D. Sun, N. Zhang, R.B. Huang, L.S. Zheng, Cryst. Growth Des. 10 (2010) 3699;
(f) Y. Zhang, J. Yang, Y. Yang, J. Guo, J.F. Ma Cryst, Growth Des. 12 (2012) 4060;
(g) L.L. Liu, Z.G. Ren, L.W. Zhu, H.F. Wang, W.Y. Yan, J.P. Lang, Cryst. Growth Des. 11 (2011) 3479;
(h) H.L. Sun, Z.M. Wang, S. Gao, S.R. Batten, CrystEngComm 10 (2008) 1796;
(i) D. Liu, Z.G. Ren, H.X. Li, Y. Chen, J. Wang, Y. Zhang, J.P. Lang, CrystEngComm 12 (2010) 1912.

[9] (a) Y. Liu, Y. Qi, Y.H. Su, F.H. Zhao, Y.X. Che, J.M. Zheng, CrystEngComm 12 (2010) 3283;
(b) P.M. Forster, N. Stock, A.K. Cheetham, Angew. Chem., Int. Ed. 44 (2005) 7608;
(c) B. Zheng, J.F. Bai, Z.X. Zhang, CrystEngComm 12 (2010) 49;
(d) L.S. Long, CrystEngComm 12 (2010) 1354;
(e) J.S. Qin, D.Y. Du, S.L. Li, Y.Q. Lan, K.Z. Shao, Z.M. Su, CrystEngComm 13 (2011) 779;
(f) H.X. Yang, S.Y. Gao, J. Lü, B. Xu, J.X. Lin, R. Cao, Inorg. Chem. 49 (2010) 736;
(g) S.M. Fang, Q. Zhang, M. Hu, E.C. Sanudo, M. Du, C.S. Liu, Inorg. Chem. 49 (2010);
(h) C.J. Shen, T.L. Sheng, C.B. Tian, Q.L. Zhu, X.T. Wu, Inorg. Chem. Commun. 17 (2012) 142.

[10] (a) J.J. Zhang, L. Wojtas, R.W. Larsen, M. Eddaoudi, M.J. Zaworotko, J. Am. Chem. Soc. 131 (2009) 17040;
(b) L.F. Ma, L.Y. Wang, D.H. Lu, S.R. Batten, J.G. Wang, Cryst. Growth Des. 9 (2009) 1741;
(c) F.J. Meng, H.Q. Jia, N.H. Hu, J.W. Xu, Inorg. Chem. Commun. 21 (2012) 186;
(d) B. Liu, G.P. Yang, Y.Y. Wang, R.T. Liu, L. Hou, Q.Z. Shi, Inorg. Chim. Acta 367 (2011) 127;
(e) H.J. Cheng, H.X. Li, Z.G. Ren, C.N. Lü, J. Shi, J.P. Lang, CrystEngComm 14 (2012) 6064.

[11] (a) J.P. Lang, Q.F. Xu, R.X. Yuan, B.F. Abrahams, Angew. Chem., Int. Ed. 43 (2004) 4741;
(b) B.C. Tzeng, T.Y. Chang, Cryst. Growth Des. 9 (2009) 5343;
(c) S.C. Chen, R.R. Qin, Z.H. Zhang, J. Qin, H.B. Gao, F.A. Sun, M.Y. He, Q. Chen, Inorg. Chim. Acta 390 (2012) 61;
(d) Y.Y. Liu, H.J. Li, Y. Han, X.F. Lv, H.W. Hou, Y.T. Fan, Cryst. Growth Des. 12 (2012) 3505.

[12] (a) M.L. Tong, S. Kitagawa, H.C. Chang, M. Ohba, Chem. Commun. (2004) 418;
(b) P. Mahata, A. Sundaresan, S. Natarajan, Chem. Commun. (2007) 4471;
(c) S. Bauer, N. Stock, Angew. Chem., Int. Ed. 46 (2007) 6857.

[13] X.M. Lin, H.C. Fang, Z.Y. Zhou, L. Chen, J.W. Zhao, S.Z. Zhu, Y.P. Cai, CrystEngComm 11 (2009) 847.

[14] (a) Z.F. Chen, Z.L. Zhang, Y.H. Tan, Y.Z. Tang, H.K. Fun, Z.Y. Zhou, B.F. Abrahams, H. Liang, CrystEngComm 10 (2008) 217;
(b) M. Meng, D.C. Zhong, T.B. Lu, CrystEngComm 13 (2011) 6794;
(c) Y.Z. Tang, Y.H. Tan, J.W. Zhu, F.M. Ji, T.T. Xiong, W.Z. Xiao, C.F. Liao Cryst, Growth Des. 8 (2008) 1801;
(d) B.L. Chen, S.Q. Ma, E.J. Hurtado, E.B. Lobkovsky, H.C. Zhou, Inorg. Chem. 46 (2007) 8490;
(e) A.J. Cairns, J.A. Perman, L. Wojtas, V.C. Kravtsov, M.H. Alkordi, M. Eddaoudi, M.J. Zaworotko, J. Am. Chem. Soc. 130 (2008) 1560;
(f) Y.G. Lee, H.R. Moon, Y.E. Cheon, M.P. Suh, Angew. Chem., Int. Ed. 47 (2008) 7741;
(g) W.L. Liu, L.H. Ye, X.F. Liu, L.M. Yuan, J.X. Jiang, C.G. Yan, CrystEngComm 10 (2008) 1395;
(h) A.J. Lan, M. Padmanabhan, K. Li, H.H. Wu, T.J. Emge, M.C. Hong, J. Li, Inorg. Chim. Acta 366 (2011) 68.

[15] M.R. Theresa, E. Mohamed, M. David, M. O'Keeffe, O.M. Yaghi, J. Am. Chem. Soc. 122 (2000) 4843.

[16] M. Xue, G.S. Zhu, Y.X. Li, X.J. Zhao, Z. Jin, E.H. Kang, S.L. Qiu, Cryst. Growth Des. 8 (2008) 2478.

[17] E.B. Reid, E.C. Pritchett, J. Org. Chem. 18 (1953) 715.

[18] G.M. Sheldrick, SHELXS-97 and SHELXL-97, University of Göettingen, Germany, Program for X-ray Crystal Structure Solution, 1997.

[19] (a) L.L. Liu, L.M. Wan, Z.G. Ren, J.P. Lang, Inorg. Chem. Commun. 14 (2011) 1069;
(b) A. Sikorski, K. Krzymiński, A. Niziołek, J. Błażejowski, Acta Crystallogr., Sect. C C61 (2005) o690.

[20] A.F. Wells, Three-dimensional Nets and Polyhedra, Wiley-Interscience, New York, 1977.

[21] A.L. Spek, J. Appl. Crystallogr. 36 (2003) 7.

[22] D. Sarma, Cryst. Growth Des. 11 (2011) 5415.

[23] J. Ma, F.L. Jiang, L. Chen, M.Y. Wu, S.Q. Zhang, K.C. Xiong, D. Han, M.C. Hong, CrystEngComm 14 (2012) 4181.

[24] X. Liu, G.C. Guo, A.Q. Wu, L.Z. Cai, J.S. Huang, Inorg. Chem. 44 (2005) 4282.